Mutagenesis of Subunit N of the *Escherichia coli* Complex I. Identification of the Initiation Codon and the Sensitivity of Mutants to Decylubiquinone†

Bilal Amarneh and Steven B. Vik*

Department of Biological Sciences, Southern Methodist University, Dallas, Texas 75275-0376

Received January 9, 2003; Revised Manuscript Received March 13, 2003

ABSTRACT: The last gene in the *nuo* operon of *Escherichia coli*, *nuoN*, encodes a membrane-bound subunit of Complex I (NADH:ubiquinone oxidoreductase). In this report, the gene for subunit N was disrupted by a 163 bp deletion in the chromosome, resulting in the loss of Complex I function, as measured by deamino-NADH oxidase activity. This activity could be recovered after transformation of the mutant strain by a plasmid that contains the previously identified *nuoN* gene and the upstream intergenic region between *nuoM* and *nuoN*. Mutagenesis of the first ATG downstream of *nuoM* led to a loss of function, indicating that this is the likely initiation codon for *nuoN*, and predicting a protein of 485 amino acids and 52 044 Da. Thirty site-specific mutations in *nuoN* at 19 different positions were constructed in a vector that expresses the full-length subunit N with both an octahistidine tag and an HA epitope tag at the carboxyl terminus. Highly conserved charged and aromatic residues were selected for mutagenesis, as well as a substitution that occurs as a secondary mutation in Leber's hereditary optic neuropathy (LHON). Membranes from the mutant strains were tested for production of subunit N by immunoblots and for NADH-linked activities. Mutants with substitutions at six different positions (K158, K217, H224, K247, Y300, and K395) had rates of deamino-NADH oxidase activity that were no more than 50% of that of the wild type and had reduced rates of proton translocation. These mutants also showed enhanced inhibition by decylubiquinone, indicating that subunit N interacts with quinones. The mutation associated with LHON, G391S, had little effect on these functions.

NADH dehydrogenases are commonly found in energy-transducing membranes as sites for the initiation of electron transport. Complex I, or NADH:ubiquinone oxidoreductase, is found in the mitochondrial membranes of many species, and also in the plasma membranes of some bacteria (for a review, see ref *1*). It typically serves three roles: (1) initiation of electron transport, (2) regeneration of NAD for the citric acid cycle, and (3) generation of the electrochemical proton gradient through translocation of protons or other cations. Other classes of NADH:quinone oxidoreductases are known to exist in microbes. ND-2 is a single-subunit enzyme, found in *Escherichia coli* (*2*) and *Saccharomyces cerevisiae* (*3*), which reduces quinones, but does not translocate ions. The NQR enzyme is a six-subunit complex found in some bacteria, including *Vibrio alginolyticus* (*4*) and *Vibrio cholerae* (*5*), which reduces quinones and translocates Na^+ ions.

Studies of Complex I in membrane vesicles from *E. coli* demonstrated that it generates an electrochemical proton gradient and is sensitive to classical inhibitors of Complex I (*6*). Later, the cloning and sequencing of the *nuo* operon confirmed that the *E. coli* enzyme is homologous to that from mammalian mitochondria (*7*). All 13 *nuo*-encoded proteins from *E. coli* (*nuoA*−*N*) have homologues in the mitochondrial enzyme, including the seven encoded by mitochondrial DNA. Subsequent studies have confirmed the presence of most if not all of the 13 subunits in purified preparations of the *E. coli* enzyme (*8*−*10*). Electron cryomicroscopy has shown that Complex I from bovine mitochondria (*11*), *Neurospora crassa* (*12*), and *E. coli* (*13*) has a peripheral arm and a membrane arm, together forming an "L" shape. The peripheral arm contains the binding site for NADH, a bound flavin mononucleotide (FMN), and five EPR-detectable Fe−S centers. The *E. coli* enzyme also contains four additional Fe−S centers that cannot be detected by EPR. The membrane arm contains no known prosthetic groups.

The seven hydrophobic *nuo* proteins that are homologous to the seven mitochondrially encoded ones in mammals are thought to make up the membrane arm in the *E. coli* enzyme. These subunits must be involved with the reduction of the lipophilic substrate ubiquinone, and are presumably part of the ion translocation mechanism. Three of the subunits, *nuoA*, *nuoJ*, and *nuoK*, have fewer than 200 amino acids, with five or fewer predicted transmembrane spans. The other four, *nuoH*, *nuoL*, *nuoM*, and *nuoN*, have 325−613 amino acids with 8−16 predicted transmembrane spans. The role of the membrane arm is particularly interesting because many of the mutations known to cause Leber's hereditary optic neuropathy (LHON)[1] map to the mitochondrial genes that encode those proteins (*14*−*16*).

Information about the H subunit has come from work done on Complex I from several different species. Studies of the

† This work was supported by grants from The Welch Foundation (N-1378) and from the Southern Methodist University University Research Council.

* To whom correspondence should be addressed: Department of Biological Sciences, 6501 Airline Rd., Southern Methodist University, Dallas, TX 75275-0376. Telephone: (214) 768-4228. Fax: (214) 768-3955. E-mail: svik@mail.smu.edu.

10.1021/bi0340346 CCC: $25.00
Published on Web 04/08/2003

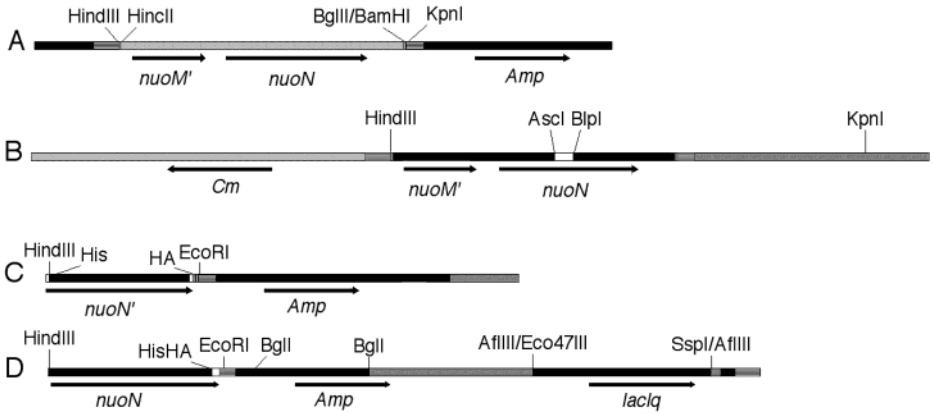

FIGURE 1: Plasmids constructed for this study. (A) A *Hin*cII−*Bgl*II fragment from pAJW104 containing part of *nuoM* and all of *nuoN* was ligated to pUC19, previously digested with *Hin*cII and *Bam*HI. This plasmid was called pBA100. (B) pBA100 was digested with *Asc*I and *Blp*I, and religated after the ends were filled using the Klenow fragment of DNA polymerase, to generate an internal deletion in *nuoN*. A *Hin*dIII−*Kpn*I fragment was then ligated to pMAK705 that was previously digested with the same enzymes. (C) Using PCR, the previously identified reading frame for *nuoN* was amplified from pBA100, incorporating a hexahistidine tag and a *Hin*dIII site at the N-terminus, and an HA tag and an *Eco*RI site at the C-terminus. The amplified gene was then ligated to pUC19 that had been previously digested with the same enzymes. This plasmid was called pBA100-N. (D) pBA200, incorporating the full-length *nuoN*, was constructed by the following three steps. First, using PCR, *nuoN* was amplified from pBA100, incorporating a *Hin*dIII site just upstream of the revised start site for *nuoN*, 180 nucleotides from the previous one. At the C-terminus, an octahistidine tag, followed by an HA tag, and an *Eco*RI site were introduced. The *Hin*dIII−*Eco*RI fragment was ligated to pUC19 that had been digested previously with the same enzymes. Second, the *lacI*^{q} gene was introduced from pMAL-c2X as an *Eco*47III−*Ssp*I fragment. It was ligated to the *nuoN* plasmid from step 1 that was previously digested with *Afl*III and whose ends were filled using the Klenow fragment of DNA polymerase. Third, the *rrnB* transcription termination region from pMAL-c2X was introduced to the region downstream of *nuoN*, using a pair of *Bgl*I sites, as indicated.

nqo8 protein, the counterpart of the *nuoH* protein from *Paracoccus denitrificans*, revealed that mutagenesis of conserved residues affected ubiquinone reduction (*17*, *18*). Furthermore, construction of a mutation in the *nqo8* subunit, which is found in the homologous mammalian subunit ND1 and is known to cause LHON, was deleterious to function in the *P. denitrificans* enzyme. Earlier work on the mitochondrial enzyme had identified the ND1 protein as a likely quinone-binding protein, because of its reaction with a photoaffinity analogue of rotenone, a quinone-like inhibitor of Complex I (*19*, *20*). The membrane topology of the homologous *nuoH* subunit from *Rhodobacter capsulatus* has been determined by the alkaline phosphatase gene fusion method, confirming the predicted eight transmembrane spans, and locating the polypeptide termini in the periplasm (*21*).

Less is known about the three largest membrane proteins, encoded by *nuoL*, *-M*, and *-N*. Sequence analysis has revealed that these three proteins are homologous (*22*), and that they are related to a family of cation antiporters (*23*). They have been predicted to have 12−16 transmembrane spans each. The L subunit from *R. capsulatus* has recently been analyzed by the alkaline phosphatase gene fusion method and found to have 14 transmembrane spans, although two additional ones might also exist (*24*). Its bovine homologue, ND5, has been shown to bind a photoaffinity analogue of Fenpyroximate, a quinone-like inhibitor of Complex I, providing the first evidence that any of these proteins interact with quinones (*25*).

This study was undertaken to probe the function of the N subunit of the *E. coli* Complex I using site-specific mutagenesis of conserved residues. In addition, a mutation associated with LHON in the homologous ND2 subunit of human Complex I was constructed in the *E. coli* system (*16*). These experiments led to the discovery that the original reading frame (*7*), encoding 425 amino acids, was incorrect, and that the actual reading frame should encode an additional 60 amino acids.

EXPERIMENTAL PROCEDURES

Materials. ACMA was obtained from Molecular Probes. Restriction enzymes and plasmid pMAL-c2X were obtained from New England BioLabs. NADH, deamino-NADH, NAD, deamino-NAD, capsaicin, and other chemicals were from Sigma Chemical Co. Nitrocellulose membranes, 12% acrylamide gels, 5-bromo-4-chloro-3-indoyl phosphate *p*-toluidine salt (BCIP), *p*-nitro blue tetrazolium chloride (NBT), and the DC protein assay were from Bio-Rad. Rat high-affinity anti-HA was from Roche. Plasmid pMAK705 (*26*) was provided by B. Cain (University of Florida, Gainesville, FL). Plasmid pAJW104 (*27*) was provided by A. J. Wolfe (Loyola University Chicago, Chicago, IL). The capsaicin analogue Cap-25 (*28*) was provided by H. Miyoshi, (Kyoto, Japan). Synthetic oligonucleotides were obtained from Operon Technologies. DNA sequencing was done by Lone Star Labs (Houston, TX).

Construction of Vectors. The vectors constructed in this study are shown in Figure 1. (A) A *Hin*cII−*Bgl*II fragment from pAJW104 containing *nuoN* and part of *nuoM* was subcloned into pUC19 at the *Hin*cII and *Bam*HI sites, generating pBA100. (B) A deletion was constructed in *nuoN* by digesting pBA100 with *Asc*I and *Blp*I, filling in the ends with deoxynucleotide triphosphates and the Klenow fragment of DNA polymerase, and ligating the blunt ends. This procedure deleted 163 bp from *nuoN*, leading to a stop codon

[1] Abbreviations: ACMA, 9-amino-6-chloro-2-methoxyacridine; BA101, *nuoN* strain; DCIP, 2,6-dichloroindophenol; EPR, electron paramagnetic resonance; FCCP, carbonyl cyanide *p*-(trifluoromethoxy)phenylhydrazone; HA epitope, mouse hemagglutinin epitope; IPTG, isopropyl β-D-thiogalactopyranoside; LHON, Leber's hereditary optic neuropathy; MES, 2-(*N*-morpholino)ethanesulfonic acid; MOPS, 3-(*N*-morpholino)-propanesulfonic acid; pBA100, plasmid for truncated *nuoN*; pBA200, plasmid for full-length *nuoN*; PCR, polymerase chain reaction; TBS, 20 mM Tris-HCl (pH 7.5) and 500 mM NaCl.

at the ligation site, and is now predicted to produce a polypeptide of 234 amino acids (*nuoN101*). A *Hin*dIII−*Kpn*I fragment containing the *nuoN101* allele was subcloned into pMAK705 in the polylinker region at those sites. (C) The plasmid called pBA100-N carries the *nuoN* gene that was proposed originally. Using PCR, this reading frame for *nuoN*, encoding 425 amino acids, was amplified from pBA100, incorporating a hexahistidine tag and a *Hin*dIII site at the N-terminus, and an HA tag and an *Eco*RI site at the C-terminus. The amplified gene was then ligated to pUC19 that was previously digested with the same enzymes. In addition to the two tags at the termini of *nuoN*, this construct differs from pBA100 in that it lacks the fragment of *nuoM* and the intergenic region between *nuoM* and -*N*. (D) pBA200, incorporating the full-length *nuoN* (485 amino acids), transcription terminators, and *lacI*^{q}, was constructed by the following three steps. First, using PCR, *nuoN* was amplified from pBA100, using the start site as the first ATG codon downstream from the end of *nuoM*. This amplified product incorporated a *Hin*dIII site just upstream of the revised start site for *nuoN*, 180 nucleotides from the previous one. At the C-terminus, an octahistidine tag, followed by an HA tag, and an *Eco*RI site were introduced. The *Hin*dIII−*Eco*RI fragment was ligated to pUC19 that was previously digested with the same enzymes. Second, the *lacI*^{q} gene was introduced from pMAL-c2X (*29*) as an *Eco*47III−*Ssp*I fragment. It was ligated to the *nuoN* plasmid from step 1 that was previously digested with *Afl*III and whose ends were filled using deoxynucleotide triphosphates and the Klenow fragment of DNA polymerase. Third, the *rrnB* transcription termination region from pMAL-c2X was introduced into the region downstream of *nuoN*, using a pair of *Bgl*I sites, as indicated.

Construction of BA101, a nuoN Strain. By homologous recombination, using the method of Hamilton et al. (*26*), a *nuoN101* strain was constructed in the background of laboratory wild-type strain 1100 (*30*). The size of the *nuoN101* deletion was confirmed to be identical in both the plasmid and the chromosome by PCR (results not shown). BA101 grew poorly on M65 minimal medium containing 25 mM acetate (*27*), but grew normally on LB medium (1% tryptone, 0.5% yeast extract, and 0.5% NaCl).

Mutagenesis. Site-specific mutations were introduced using PCR with a two-primer approach, made feasible by the numerous restriction sites in *nuoN*. The amplified fragments were subcloned back into pBA200, and the sequences of the entire fragments were verified by DNA sequencing.

Growth of Cultures and Preparation of Membrane Vesicles. Cells were grown in rich medium containing 3% tryptone, 1.5% yeast extract, 0.15% NaCl, and 1% (v/v) glycerol at 37 °C. Ampicillin was added at 0.1 g/L to cells harboring the expression plasmid. Cells grown overnight at 30 °C were used to inoculate 100 mL of culture. Induction with IPTG was done at an A_{600} of 0.6, and the cultures were harvested at an A_{600} of 1.85. As was originally reported by Matsushita et al. (*6*), Complex I activity is quite labile, and it was necessary to resuspend the cells in buffer at low pH with limited washing to preserve complex I function. The cells were harvested, resuspended in 50 mM MES, 25% glycerol, and 10 mM $MgSO_4$ (pH 6.0), and passed through the French press at 8000 psi. The supernatant fraction after a low-speed centrifugation (2 min at 15000*g*) was centrifuged at 250000*g* for 20 min. The pellet was resuspended in the same buffer, and enzyme assays were carried out the same day.

Enzyme Assays. All assays were performed in 50 mM MOPS and 10 mM $MgCl_2$ (pH 7.3) at 21 °C with 0.25 mM deamino-NADH or NADH. The assay medium also included FCCP at 1 μM. Deamino-NADH oxidase activity was assayed using either oxygen or DCIP (60 μM) as the terminal electron acceptor, using a Beckman DU 650 spectrophotometer. The extinction coefficients that were used were 6.22 mM^{-1} cm^{-1} for NADH and deamino-NADH and 20.6 mM^{-1} cm^{-1} for DCIP. Complex I inhibitor capsaicin and a synthetic analogue (Cap-25) were added at 0.3 and 0.1 mM, respectively, followed by incubation for 1 min before addition of the substrates. The inhibitors were equally effective. Decylubiquinone was added to the deamino-NADH oxidase assay at 0.25 mM. Proton translocation was assayed by measuring the fluorescence quenching of ACMA (10 μM) in 50 mM MOPS and 10 mM $MgCl_2$ (pH 7.3) at 21 °C with 0.1 mM deamino-NADH. Membrane protein was added to a final concentration of 75 mg/L.

Immunoblotting. Fifty micrograms of protein from membrane fractions was subjected to SDS−PAGE using 12% acrylamide gels. The proteins were transblotted onto nitrocellulose membranes. Membranes were blocked in TBS containing 5% fat free milk, washed three times in TBS containing 0.1% Tween 20, and incubated in a high-affinity anti-HA rat monoclonal antibody (Roche). The nitrocellulose membrane was washed, and the goat anti-rat antibody coupled to alkaline phosphatase was added. After incubation, the blot was washed and developed with NBT/BCIP.

RESULTS

The *nuoN* strain, BA101, constructed in this study showed the expected slow growth phenotype on minimal medium containing acetate as the sole carbon source, indicative of the lack of Complex I function (*27*). Initial attempts to complement this strain with a plasmid expressing *nuoN*, as described in the literature (*7*), met with failure. The vector shown in Figure 1C was one of several constructs tested that contained the reported gene that encodes a protein of 425 amino acids. Eventually, inspection of the upstream region of the *nuoN* gene revealed that there were two additional, in-frame, methionine codons, and that all three had potential Shine-Dalgarno sequences, as indicated by analysis of Schultzaburger et al. (*31*). Figure 2 shows that the first methionine codon is six nucleotides from the predicted stop codon of *nuoM*. The vector pBA200 was constructed, shown in Figure 1D, which includes the first of the three potential start codons, and it led to wild-type function when the BA101 strain (*nuoN*$^-$) was transformed with it (results presented later). To test the possible role of this methionine as an initiation codon, the ATG codon was changed to CAT (histidine). This mutation had deleterious effects on function (results presented later).

Complementation by the full-length *nuoN* vector, pBA200, was verified by a series of NADH-driven assays, as shown in Table 1. *E. coli* normally produces two types of NADH: quinone oxidoreductases, Complex I and NDH-2 (*6*, *32*). They can be distinguished because only Complex I is sensitive to capsaicin (*33*) and only Complex I can utilize deamino-NADH as a substrate (*6*). As indicated in Table 1,

Table 1: Activities[a] of Membrane Vesicles from Mutant, Wild-Type, and Complemented Strains

strain	NADH oxidase		deamino-NADH oxidase		deamino-NADH/ DCIP reductase	
	without capsaicin	with capsaicin[b]	without capsaicin	with capsaicin[b]	without capsaicin	with capsaicin[b]
BA101 (*nuoN*$^-$)	450	420	0	0	80	70
1100 (wild type)	710	320	450	30	100	80
BA101/pBA200	680	330	460	35	100	80

[a] Activities are in nanomoles per milligram per minute. Values are the averages of two measurements that did not differ from the mean by more than 10%. [b] With 300 μM capsaicin.

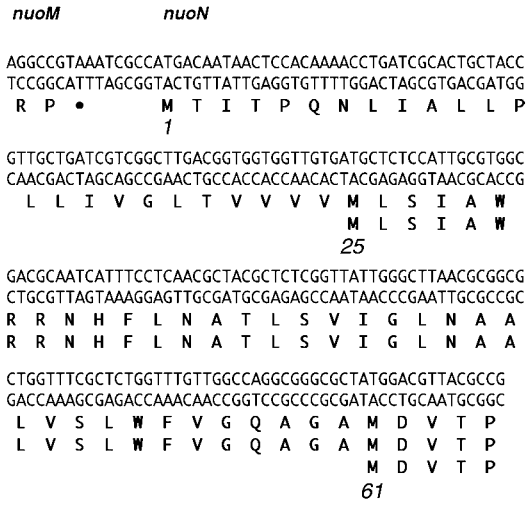

FIGURE 2: Three possible start sites for *nuoN*. The previously identified start site for *nuoN* is the one labeled 61. The proposed start site is the one labeled 1, closest to the predicted stop codon for *nuoM*. A third methionine codon can be found in-frame at position 25.

in wild-type cells, ~60% of the NADH oxidase activity is due to Complex I. This activity is completely absent in BA101, the *nuoN*$^-$ strain. Considerable deamino-NADH: DCIP reductase activity is retained, indicating partial assembly of Complex I on the membranes. When BA101 is transformed with pBA200, the full-length *nuoN* vector, the rates are virtually the same as that of the wild type.

Using the pBA200 vector, 28 substitution mutations were constructed, along with two additional ones that were generated by PCR mistakes, and all are listed in Table 2. Seventeen highly conserved positions were selected, including glutamic acid, arginine, lysine, histidine, tyrosine, and tryptophan. In addition, G391S was constructed because it is a mutation that occurs in LHON, although it is thought not to be sufficient to cause the disease (*16*). All mutations were tested for the level of protein after induction in BA101, using the engineered HA epitope in an immunoblot, and the results are shown in Figure 3. In panel A, detection of the full-length version (called wt) can be compared with the ATG to CAT substitution (M1H), and with the construct that begins with M61. The last lane shows that without induction, no expression is detected. In panels B−D of Figure 3, the immunoblots of 18 substitution mutants are shown. The only mutant that produced no detectable N subunit was K217C, shown in lane 1 of panel B. All other mutants, including those not shown, were detected at levels similar to that of the wild-type protein.

All mutants were tested for deamino-NADH oxidase activity in preparations of membrane vesicles, and the results

Table 2: Deamino-NADH Oxidase Activity of Mutants and Sensitivity to Decylubiquinone

construct	deamino-NADH oxidase[a]	deamino-NADH oxidase with decylubiquinone[b]
wild type	1.0	+++
ΔM61	0.05	ND[c]
M1H	0.2	+++
M74K	0.9	+++
C88S	1.0	+++
C88V	1.0	+++
E104C	0.9	+++
E133A	0.7	+++
E133C	0.7	+++
E133D	0.8	+++
R151C	0.9	+++
E154C	0.7	±
K158C	0.5	− − −
K158R	0.7	+
T160I	0.8	+++
K217C	0	ND[c]
K217R	0.4	++
H224A	1.0	+++
H224Y	0.9	+++
H224K	0.4	− −
W226C	0.9	+++
D229C	0.7	+++
K247C	0.07	ND[c]
K247R	0.8	+++
K295C	0.8	+++
K295R	0.9	+++
Y300C	0.7	±
Y300S	0.5	±
G391S	0.9	+++
K395C	0.05	ND[c]
K395R	0.3	++
Y424C	0.9	+++
M482C	1.0	+++

[a] The assays were carried out in 50 mM MOPS, 10 mM $MgCl_2$, and 1 μM FCCP at pH 7.3 and 21 °C. Deamino-NADH was added at a concentration of 250 μM. Values are the averages of two to five measurements, which did not differ from the mean by more than 10%. [b] Decylubiquinone was added at a concentration of 250 μM. +++ indicates a stimulation of 30−60%. ++ indicates a stimulation of 10−30%. + indicates a stimulation of 0−10%. The negative signs indicate inhibition to the corresponding degree. ± indicates no stimulation. [c] Not determined due to a very low level of activity.

are shown in Table 2. Assays were carried out in the presence of 1 μM FCCP to prevent inhibition of electron transport due to the buildup of a proton gradient. The construct M61, which produces a subunit N lacking the first 60 amino acids, has only 5% of the wild-type rate of deamino-NADH oxidase, consistent with its low level of protein detected by immunoblots in Figure 3A. Membranes from M1H exhibit ~20% of the wild-type rate of deamino-NADH oxidase, also consistent with the low level of protein seen in Figure 3A. Membranes prepared from K217C showed no activity, as expected, since no subunit N was detected by immunoblots

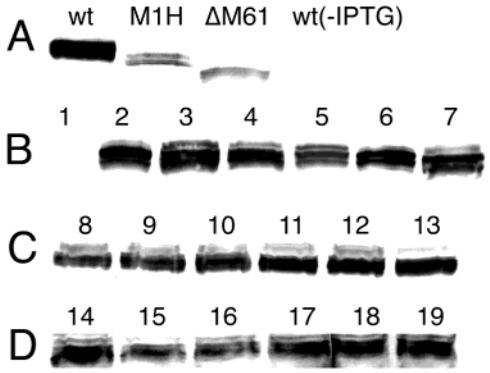

FIGURE 3: Immunoblots of subunit N expressed from plasmids. Samples were taken from preparations of membrane vesicles. Subunit N was detected with a monoclonal antibody against the HA epitope. (A) The first lane contained wild-type (wt) plasmid pBA200. The second lane contained the N-terminal mutant, M1H. The third lane, ΔM61, contained the original construct pBA100 that lacks the first 60 amino acids of subunit N. The last lane is the same as the first lane, but without induction with IPTG. All other lanes contained cells induced with IPTG. (B) Lane 1 contained K217C, lane 2 K395R, lane 3 K158C, lane 4 K295C, lane 5 G391S, lane 6 H224Y, and lane 7 E133C. (C) Lane 9 contained the wild type, lane 10 W226C, lane 10 K217R, lane 11 K247C, lane 12 H224K, and lane 13 E154C. (D) Lane 14 contained Y424C, lane 15 contained K395C, lane 16 contained Y300S, lane 17 contained Y300C, lane 18 contained K158R, and lane 19 contained R151C.

(Figure 3B). All of the other substitution mutants were intermediate with respect to deamino-NADH oxidase activity. In particular, mutations at residues K217, H224, K247, and K395 resulted in rates of deamino-NADH oxidase that were below 50% of the wild-type rate. The deamino-NADH oxidase rates of all mutants were also measured in the presence of 300 μM capsaicin, which inhibited the wild type by ~90% (Table 1). No significant differences in the level of inhibition were seen. Membranes from K247C and K395C, which had especially low rates of deamino-NADH oxidase activity, were tested further for deamino-NADH/DCIP reductase activity as an indicator of assembly. K247C had rates similar to that of the *nuoN* strain BA101, suggesting only partial assembly, while K395C was similar to the wild type, suggesting normal assembly.

All mutants were also tested for the effect of exogenous decylubiquinone on the rate of deamino-NADH oxidase activity. When added at a level of 0.25 mM to wild-type membranes, the rate was stimulated typically 30−60%. This is indicated by +++ in Table 2. In contrast, two mutants were inhibited by this level of decylubiquinone. Membranes from K158C were inhibited by 30−50%, and membranes from H224K were inhibited by 20−30%. Others showed marginal stimulation (K158R and K217R) or little effect (E154C, Y300S, and Y300C) upon addition of decylubiquinone to the assay medium. To investigate this inhibition further, three mutants were selected to be assayed at three different concentrations of decylubiquinone, and the results are shown in Figure 4. The wild-type membranes show stimulation at low concentrations of decylubiquinone. Membranes from Y300S show only marginal stimulation at 80 μM decylubiquinone, while the other two, H224K and K158C, show inhibition at all concentrations that were tested.

Finally, all mutants were tested for rates of proton translocation, and the results are shown in Figure 5. Deamino-NADH was added to membrane vesicles in the presence of the fluorescent dye ACMA, and proton translocation is indicated by the quenching of the fluorescence.

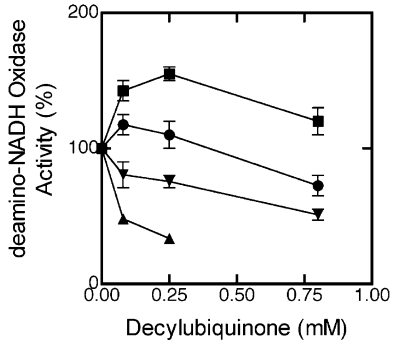

FIGURE 4: Effect of decylubiquinone on the deamino-NADH oxidase activity. Membrane vesicles were prepared from the wild type (■) and three mutants: Y300S (●), H224K (▼), and K158C (▲). Assays were conducted in the presence of 250 μM deamino-NADH and the indicated concentration of decylubiquinone. Rates in the presence of decylubiquinone are expressed as a percentage of the rate in its absence. Rates are the average of activities from two independent preparations, and the standard errors are indicated by bars.

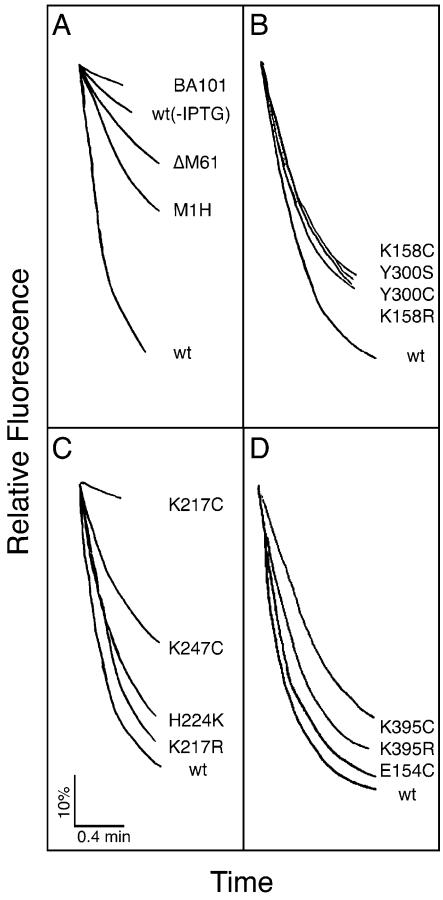

FIGURE 5: Proton translocation assays of the *nuoN* mutants. Membrane vesicles were prepared from each of the indicated mutants, and the extent of proton translocation was measured by the quenching of the fluorescence of ACMA after addition of deamino-NADH. (A) wt indicates the wild-type subunit N expressed from pBA200. M1H is the mutation of the N-terminal residue to histidine. ΔM61 is the original construct pBA100, lacking the first 60 amino acids of subunit N. wt(−IPTG) is the wild-type subunit N without induction by IPTG. BA101 is the *nuoN*$^-$ strain. In panels B−D, other mutants are analyzed. The traces that are shown are representative of those obtained from two to five independent preparations of membranes.

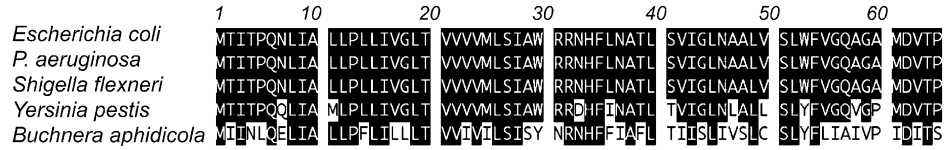

FIGURE 6: Conservation of the N-terminal region of subunit N. The predicted N-terminal residues of subunit N from *E. coli* [GenBank entry P33608 (*41*)] are compared with those from *Pseudomonas aeruginosa* [GenBankentry (*42*)], *Shigella flexneri* [GenBank entry NP_708158 (*43*)], *Yersinia pestis* [GenBank entry Q8ZDL9 (*44*)], and *Buchnera aphidicola* [GenBank entry Q8K9X5 (*45*)]. The shading indicates residues that are identical to the *E. coli* sequence.

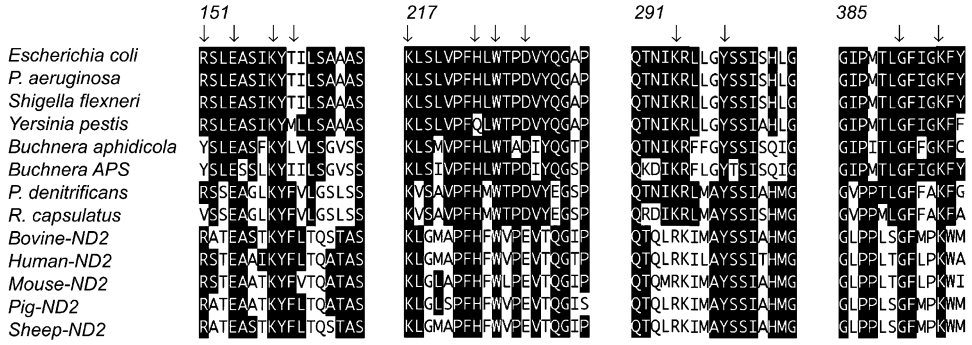

FIGURE 7: Four conserved regions of subunit N. In addition to that from *E. coli*, seven sequences from other bacteria are shown, and sequences from five mammalian mitochondrial sources are included. The shading indicates residues that are identical to the *E. coli* sequence. The sites of mutations analyzed in this study are indicated by arrows. In the first segment (residues 151−167), mutants R151C, E154C, K158C, K158R, and T160I were constructed. In the second segment (residues 217−235), mutants K217C, K217R, H224A, H224Y, H224K, W226C, and D229C were constructed. In the third segment (residues 291−307), mutants K295C, K295R, Y300C, and Y300S were constructed. In the fourth segment (residues 385−397), G391S, K395C, and K395R were constructed. The following sequences were not referenced in Figure 6: *Buchnera* APS [GenBank entry P57264 (*46*)], *P. denitrificans* [GenBank entry P29926 (*47*)], *R. capsulatus* [GenBank entry P50973 (*48*)], bovine [GenBank entry P03892 (*49*)], human [GenBank entry P03891 (*49*)], mouse [GenBank entry P03893 (*50*)], pig [GenBank entry O79875 (*51*)], and sheep [GenBank entry O78748 (*52*)].

In panel *A*, the wild-type strain showed rapid proton translocation, while the *nuoN*$^-$ strain, BA101, showed very little quenching. Without induction by IPTG, BA101 carrying a wild-type *nuoN* on the plasmid pBA200 had only marginally more quenching. The N-terminal mutants, ΔM61 and M1H, showed slightly higher rates of proton translocation, but rates much lower than the wild-type rate. In panel B, four mutants that exhibit 50−70% of the wild-type rate of deamino-NADH oxidase activity are assayed for proton translocation. All show similarly diminished rates of proton translocation. In panels C and D, seven other mutants are analyzed. Membranes from K217C, which were shown to lack subunit N, showed no evidence of proton translocation, as expected. Membranes from K247C had greatly diminished rates of proton translocation, while those from H224K, K247R, K217R, K395C, K395R, and E154C were all somewhat lower than the wild-type rate, to various degrees. Other mutants listed in Table 2, but not shown in Figure 5, had rates of proton translocation that were indistinguishable from that of the wild type.

DISCUSSION

The *nuo* operon from *E. coli* contains 13 genes (*7*), and purified preparations of Complex I have been shown to contain 13 protein subunits (*8*−*10*). Some of the subunits have been identified by N-terminal amino acid sequencing, which also provides information about the start sites of protein synthesis. In the study presented here, evidence is presented that the previously recognized start site for *nuoN* is 180 nucleotides downstream of the actual start site. Three lines of evidence are provided. First, membranes from cells that expressed only the recognized sequence (Figure 1C) had very little N subunit, and very low deamino-NADH oxidase activity. Second, membranes from cells with a vector that included the 180 nucleotides upstream (Figure 1D) had properties similar to those of the wild-type strain. Mutagenesis of the first codon to histidine, M1H, resulted in low protein levels and greatly inhibited function. Third, a comparison of several other bacterial *nuo* sequences, shown in Figure 6, reveals that this segment of 60 amino acids is highly conserved. Therefore, it is likely that the *nuoN* gene in *E. coli* encodes a protein of 485 amino acids and ∼52 kDa.

Subunit N is one of the three large, hydrophobic proteins of Complex I that are homologous to each other. No function has been identified with these subunits, but sequence similarity has been noted to cation antiporters. In this study, 18 highly conserved residues were identified for mutagenesis. These residues included charged and aromatic residues, many of which appeared in clusters. Four such segments are shown in Figure 7, with sites of mutagenesis indicated by arrows. The aligned sequences include both bacterial and mammalian sequences, demonstrating the widespread conservation of the selected residues.

Mutations at four different sites led to rates of deamino-NADH oxidase below 50% of the wild-type rate. In particular, K395C of the fourth segment in Figure 7 exhibited only 5% of the wild-type rate, and K247C (not shown in Figure 7) exhibited only 7% of the wild-type rate. Others were K217R (40%), H224K (40%), and K395R (30%). Among these, H224K was striking in that its rate was not stimulated by exogenous decylubiquinone, but rather was inhibited, even at the lowest concentration. K158C was similar in this regard.

Complex I has been shown to be stimulated by soluble quinones at lower concentrations, and inhibited at higher

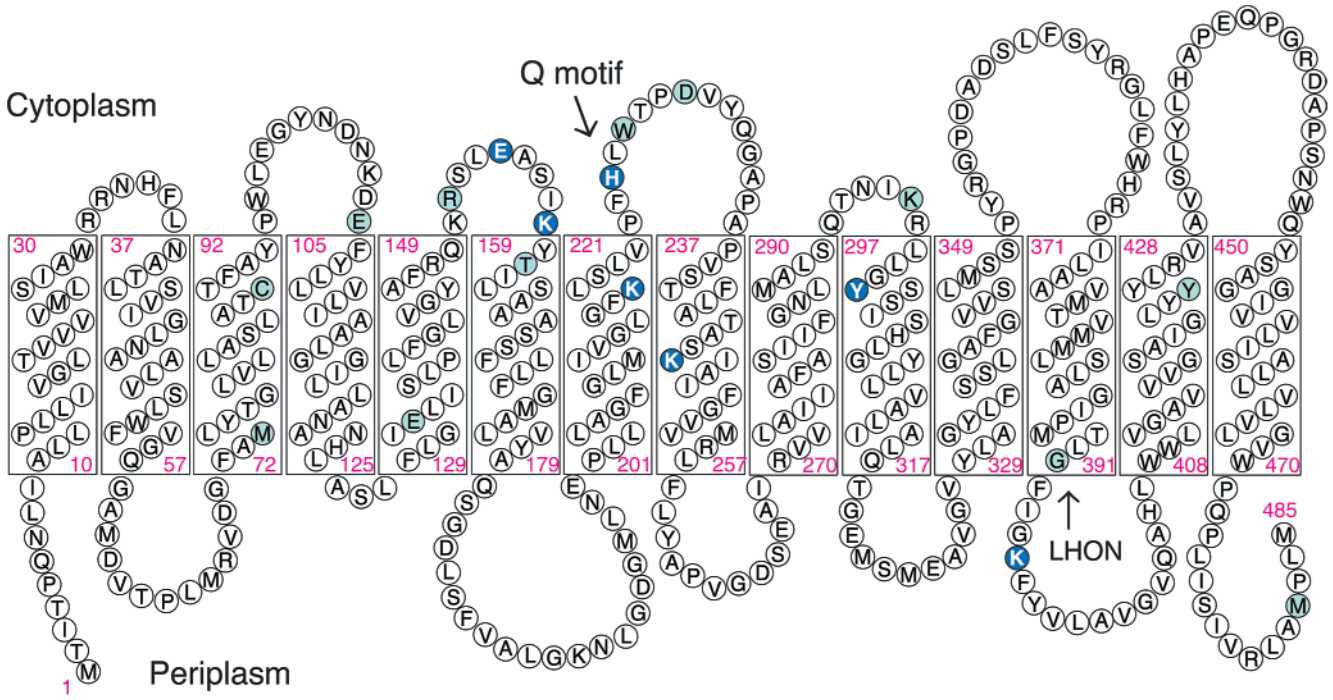

FIGURE 8: Transmembrane model of subunit N. The mutations used in this study are indicated by the color blue. Lighter blue indicates that the mutation had little or no effect on function. Darker blue indicates that the mutation caused a ≥50% reduction in deamino-NADH oxidase activity, or that decylubiquinone was not as stimulatory as with the wild type. Most of the deleterious mutations are found near the predicted cytoplasmic surface, in the central region of the polypeptide chain. A notable exception is K395, which is near the LHON site and appears to be in the periplasm. This model is similar to one in a recently published study (*24*), except for the location of the region in subunit N between residues 297 and 349, which was removed from the bilayer.

concentrations (*34*, *35*). The simplest interpretation of this observation is that the soluble quinones bind with high affinity to "quinone" sites, and with low affinity to "quinone-intermediate" sites. Since quinone reduction is a two-electron, two-proton reaction, there are likely to be binding sites for intermediates to facilitate proton translocation. The observation here that several mutants have enhanced inhibition by decylubiquinone argues that subunit N contains a binding site for a quinone intermediate. These particular substitutions might strengthen the binding of decylubiquinone, e.g., K158C, or alternatively, they might allow access of the bulk soluble quinones to the binding site by disrupting the protein structure.

A quinone-binding motif has been proposed for respiratory complexes by Fisher and Rich (*36*). In the second segment of Figure 7, labeled residue 217, a motif of the type L-(X_3)-H-(X_2)-T, can be detected starting with L220 of the *E. coli* sequence. This motif is present throughout the bacterial sequences, with one exception. Among the mammalian sequences, the first part of the motif is conserved, but the threonine is missing in each case. This motif is not conserved among *nuoL* or *nuoM*, even in *E. coli*.

The ability of each mutant to build a proton gradient was also assessed. In general, one might expect either that the extent of deamino-NADH oxidase and proton translocation would decrease together or that the extent of proton translocation would decrease more than that of deamino-NADH oxidase. Since it is thought that electron transport drives proton translocation, one would not expect to find mutants in which the rate of electron transport is reduced, but proton translocation is normal. When attempting to compare the rates of electron transport in Table 2 with the rates of proton translocation in Figure 5, one should note that the rates of fluorescence quenching are not exactly proportional to the rates of proton translocation. For example, K395C exhibits ~5% of the wild-type rate of electron transport (Table 2), while it exhibits an apparent rate of proton translocation that is ~30% of the wild-type rate. The mutants K247C and H224K in Figure 5C, K395C and K395R in Figure 5D, and K158C, K158R, Y300S, and Y300C in Figure 5B have relatively slower rates of proton translocation. Since the latter four mutants have much higher rates of deamino-NADH oxidase activity than the other four mutants, it suggests that residues K158 and Y300 might be at or near sites critical to proton translocation. Other evidence indicates that the *E. coli* Complex I might also translocate Na^+ ions (*37*), and it has been shown that the purified Complex I from *Klebsiella pneumoniae* does (*38*, *39*). In the case of subunit N, the amino acid sequences are 93% identical between the two, and all of the conserved residues tested in this study are identical. In any case, it is likely that protons are taken up vectorially, from the cytoplasm, to generate quinols from quinones.

The results of this study are summarized in the transmembrane model of subunit N in Figure 8. It is based on the TMHMM (transmembrane hidden Markov model) prediction of transmembrane spans (*40*), and considerations of hydropathy and sequence conservation. The 14 transmembrane spans are arranged with the two termini in the periplasm. Sites of mutations that cause increased sensitivity to decylubiquinone, or that cause greatly reduced deamino-NADH oxidase activity, are represented by dark blue circles. Those with minimal or no effect are a lighter shade of blue. Most of the critical residues are found in the central part of the protein, near the quinone motif. We propose that the central region of subunit N, residues 150−300, binds a quinone

intermediate, which is protonated from the cytoplasmic surface. Since no variation in capsaicin sensitivity was seen, it is likely that subunit N does not bind this inhibitor.

One other critical residue is K395, which is predicted to face the periplasm. This conserved residue is near G391, the residue found to be serine in some cases of LHON (*16*). In *E. coli*, the G391S mutant behaved in a manner nearly identical to that of the wild type in our study, and therefore provided no insight into the possible deleterious effects in humans. However, the mutations at K395 had greatly reduced rates of deamino-NADH oxidase activity, indicating that this might be a critical region of the protein.

ACKNOWLEDGMENT

We thank Dr. Alan J. Wolfe for generously providing plasmid pAJW104, Dr. Brian Cain for generously providing pMAK705, and Dr. Hideo Miyoshi for generously providing capsaicin analogue Cap-25.

REFERENCES

1. Walker, J. E. (1992) The NADH:ubiquinone oxidoreductase (complex I) of respiratory chains, *Q. Rev. Biophys. 25*, 253−324.
2. Bjorklof, K., Zickermann, V., and Finel, M. (2000) Purification of the 45 kDa, membrane bound NADH dehydrogenase of *Escherichia coli* (NDH-2) and analysis of its interaction with ubiquinone analogues, *FEBS Lett. 467*, 105−110.
3. de Vries, S., and Grivell, L. A. (1988) Purification and characterization of a rotenone-insensitive NADH:Q6 oxidoreductase from mitochondria of *Saccharomyces cerevisiae*, *Eur. J. Biochem. 176*, 377−384.
4. Nakayama, Y., Hayashi, M., and Unemoto, T. (1998) Identification of six subunits constituting Na^+-translocating NADH-quinone reductase from the marine *Vibrio alginolyticus*, *FEBS Lett. 422*, 240−242.
5. Barquera, B., Hellwig, P., Zhou, W., Morgan, J. E., Hase, C. C., Gosink, K. K., Nilges, M., Bruesehoff, P. J., Roth, A., Lancaster, C. R., and Gennis, R. B. (2002) Purification and characterization of the recombinant Na^+-translocating NADH:quinone oxidoreductase from *Vibrio cholerae*, *Biochemistry 41*, 3781−3789.
6. Matsushita, K., Ohnishi, T., and Kaback, H. R. (1987) NADH-ubiquinone oxidoreductases of the *Escherichia coli* aerobic respiratory chain, *Biochemistry 26*, 7732−7737.
7. Weidner, U., Geier, S., Ptock, A., Friedrich, T., Leif, H., and Weiss, H. (1993) The gene locus of the proton-translocating NADH: ubiquinone oxidoreductase in *Escherichia coli*. Organization of the 14 genes and relationship between the derived proteins and subunits of mitochondrial complex I, *J. Mol. Biol. 233*, 109−122.
8. Spehr, V., Schlitt, A., Scheide, D., Guenebaut, V., and Friedrich, T. (1999) Overexpression of the *Escherichia coli nuo*-operon and isolation of the overproduced NADH:ubiquinone oxidoreductase (complex I), *Biochemistry 38*, 16261−16267.
9. David, P., Baumann, M., Wikström, M., and Finel, M. (2002) Interaction of purified NDH-1 from *Escherichia coli* with ubiquinone analogues, *Biochim. Biophys. Acta 1553*, 268−278.
10. Leif, H., Sled, V. D., Ohnishi, T., Weiss, H., and Friedrich, T. (1995) Isolation and characterization of the proton-translocating NADH: ubiquinone oxidoreductase from *Escherichia coli*, *Eur. J. Biochem. 230*, 538−548.
11. Grigorieff, N. (1998) Three-dimensional structure of bovine NADH:Ubiquinone oxidoreductase (Complex I) at 22 Å in ice, *J. Mol. Biol. 277*, 1033−1046.
12. Leonard, K., Haiker, H., and Weiss, H. (1987) Three-dimensional structure of NADH:ubiquinone reductase (complex I) from *Neurospora* mitochondria determined by electron microscopy of membrane crystals, *J. Mol. Biol. 194*, 277−286.
13. Guenebaut, V., Schlitt, A., Weiss, H., Leonard, K., and Friedrich, T. (1998) Consistent structure between bacterial and mitochondrial NADH:ubiquinone oxidoreductase (complex I), *J. Mol. Biol. 276*, 105−112.
14. Howell, N., Bindoff, L. A., McCullough, D. A., Kubacka, I., Poulton, J., Mackey, D., Taylor, L., and Turnbull, D. M. (1991) Leber hereditary optic neuropathy: identification of the same mitochondrial ND1 mutation in six pedigrees, *Am. J. Hum. Genet. 49*, 939−950.
15. Chinnery, P. F., Brown, D. T., Andrews, R. M., Singh-Kler, R., Riordan-Eva, P., Lindley, J., Applegarth, D. A., Turnbull, D. M., and Howell, N. (2001) The mitochondrial ND6 gene is a hot spot for mutations that cause Leber's hereditary optic neuropathy, *Brain 124*, 209−218.
16. Brown, M. D., Voljavec, A. S., Lott, M. T., Torroni, A., Yang, C. C., and Wallace, D. C. (1992) Mitochondrial DNA complex I and III mutations associated with Leber's hereditary optic neuropathy, *Genetics 130*, 163−173.
17. Zickermann, V., Barquera, B., Wikström, M., and Finel, M. (1998) Analysis of the pathogenic human mitochondrial mutation ND1/3460, and mutations of strictly conserved residues in its vicinity, using the bacterium *Paracoccus denitrificans*, *Biochemistry 37*, 11792−11796.
18. Kurki, S., Zickermann, V., Kervinen, M., Hassinen, I., and Finel, M. (2000) Mutagenesis of three conserved Glu residues in a bacterial homologue of the ND1 subunit of complex I affects ubiquinone reduction kinetics but not inhibition by dicyclohexylcarbodiimide, *Biochemistry 39*, 13496−13502.
19. Earley, F. G., and Ragan, C. I. (1984) Photoaffinity labelling of mitochondrial NADH dehydrogenase with arylazidoamorphigenin, an analogue of rotenone, *Biochem. J. 224*, 525−534.
20. Earley, F. G., Patel, S. D., Ragan, I., and Attardi, G. (1987) Photolabelling of a mitochondrially encoded subunit of NADH dehydrogenase with [^{3}H]dihydrorotenone, *FEBS Lett. 219*, 108−112.
21. Roth, R., and Hägerhäll, C. (2001) Transmembrane orientation and topology of the NADH:quinone oxidoreductase putative quinone binding subunit NuoH, *Biochim. Biophys. Acta 1504*, 352−362.
22. Fearnley, I. M., and Walker, J. E. (1992) Conservation of sequences of subunits of mitochondrial complex I and their relationships with other proteins, *Biochim. Biophys. Acta 1140*, 105−134.
23. Friedrich, T., and Weiss, H. (1997) Modular evolution of the respiratory NADH:ubiquinone oxidoreductase and the origin of its modules, *J. Theor. Biol. 187*, 529−540.
24. Mathiesen, C., and Hägerhäll, C. (2002) Transmembrane topology of the NuoL, M and N subunits of NADH:quinone oxidoreductase and their homologues among membrane-bound hydrogenases and bona fide antiporters, *Biochim. Biophys. Acta 1556*, 121−132.
25. Nakamaru-Ogiso, E., Sakamoto, K., Matsuno-Yagi, A., Miyoshi, H., and Yagi, T. (2003) The ND5 subunit was labeled by a photoaffinity analogue of Fenpyroximate in bovine mitochondrial Complex I, *Biochemistry 42*, 746−754.
26. Hamilton, C. M., Aldea, M., Washburn, B. K., Babitzke, P., and Kushner, S. R. (1989) New method for generating deletions and gene replacements in *Escherichia coli*, *J. Bacteriol. 171*, 4617−4622.
27. Pruess, B. M., Nelms, J. M., Park, C., and Wolfe, A. J. (1994) Mutations in NADH:ubiquinone oxidoreductase of *Escherichia coli* affect growth on mixed amino acids, *J. Bacteriol. 176*, 2143−2150.
28. Satoh, T., Miyoshi, H., Sakamoto, K., and Iwamura, H. (1996) Comparison of the inhibitory action of synthetic capsaicin analogues with various NADH-ubiquinone oxidoreductases, *Biochim. Biophys. Acta 1273*, 21−30.
29. Guan, C. D., Li, P., Riggs, P. D., and Inouye, H. (1988) Vectors that facilitate the expression and purification of foreign peptides in *Escherichia coli* by fusion to maltose-binding protein, *Gene 67*, 21−30.
30. Humbert, R., Brusilow, W. S., Gunsalus, R. P., Klionsky, D. J., and Simoni, R. D. (1983) *Escherichia coli* mutants defective in the uncH gene, *J. Bacteriol. 153*, 416−422.
31. Shultzaberger, R. K., Bucheimer, R. E., Rudd, K. E., and Schneider, T. D. (2001) Anatomy of *Escherichia coli* ribosome binding sites, *J. Mol. Biol. 313*, 215−228.
32. Calhoun, M. W., Oden, K. L., Gennis, R. B., de Mattos, M. J., and Neijssel, O. M. (1993) Energetic efficiency of *Escherichia coli*: effects of mutations in components of the aerobic respiratory chain, *J. Bacteriol. 175*, 3020−3025.
33. Yagi, T. (1990) Inhibition by capsaicin of NADH-quinone oxidoreductases is correlated with the presence of energy-coupling site 1 in various organisms, *Arch. Biochem. Biophys. 281*, 305−311.

34. Helfenbaum, L., Ngo, A., Ghelli, A., Linnane, A. W., and Esposti, M. D. (1997) Proton pumping of mitochondrial complex I: Differential activation by analogs of ubiquinone, *J. Bioenerg. Biomembr. 29*, 71−80.
35. Esposti, M. D., Ngo, A., McMullen, G. L., Ghelli, A., Sparla, F., Benelli, B., Ratta, M., and Linnane, A. W. (1996) The specificity of mitochondrial complex I for ubiquinones, *Biochem. J. 313*, 327−334.
36. Fisher, N., and Rich, P. R. (2000) A motif for quinone binding sites in respiratory and photosynthetic systems, *J. Mol. Biol. 296*, 1153−1162.
37. Steuber, J., Schmid, C., Rufibach, M., and Dimroth, P. (2000) Na^+ translocation by complex I (NADH:quinone oxidoreductase) of *Escherichia coli*, *Mol. Microbiol. 35*, 428−434.
38. Krebs, W., Steuber, J., Gemperli, A. C., and Dimroth, P. (1999) Na^+ translocation by the NADH:ubiquinone oxidoreductase (complex I) from *Klebsiella pneumoniae*, *Mol. Microbiol. 33*, 590−598.
39. Gemperli, A. C., Dimroth, P., and Steuber, J. (2002) The respiratory complex I (NDH I) from *Klebsiella pneumoniae*, a sodium pump, *J. Biol. Chem. 277*, 33811−33817.
40. Krogh, A., Larsson, B., von Heijne, G., and Sonnhammer, E. L. (2001) Predicting transmembrane protein topology with a hidden Markov model: application to complete genomes, *J. Mol. Biol. 305*, 567−580.
41. Blattner, F. R., Plunkett, G., III, Bloch, C. A., Perna, N. T., Burland, V., Riley, M., Collado-Vides, J., Glasner, J. D., Rode, C. K., Mayhew, G. F., Gregor, J., Davis, N. W., Kirkpatrick, H. A., Goeden, M. A., Rose, D. J., Mau, B., and Shao, Y. (1997) The complete genome sequence of *Escherichia coli* K-12, *Science 277*, 1453−1474.
42. Stover, C. K., Pham, X. Q., Erwin, A. L., Mizoguchi, S. D., Warrener, P., Hickey, M. J., Brinkman, F. S., Hufnagle, W. O., Kowalik, D. J., Lagrou, M., Garber, R. L., Goltry, L., Tolentino, E., Westbrock-Wadman, S., Yuan, Y., Brody, L. L., Coulter, S. N., Folger, K. R., Kas, A., Larbig, K., Lim, R., Smith, K., Spencer, D., Wong, G. K., Wu, Z., Paulsen, I. T., Reizer, J., Saier, M. H., Hancock, R. E., Lory, S., and Olson, M. V. (2000) Complete genome sequence of *Pseudomonas aeruginosa* PA01, an opportunistic pathogen, *Nature 406*, 959−964.
43. Jin, Q., Yuan, Z., Xu, J., Wang, Y., Shen, Y., Lu, W., Wang, J., Liu, H., Yang, J., Yang, F., Zhang, X., Zhang, J., Yang, G., Wu, H., Qu, D., Dong, J., Sun, L., Xue, Y., Zhao, A., Gao, Y., Zhu, J., Kan, B., Ding, K., Chen, S., Cheng, H., Yao, Z., He, B., Chen, R., Ma, D., Qiang, B., Wen, Y., Hou, Y., and Yu, J. (2002) Genome sequence of *Shigella flexneri* 2a: insights into pathogenicity through comparison with genomes of *Escherichia coli* K12 and O157, *Nucleic Acids Res. 30*, 4432−4441.
44. Parkhill, J., Wren, B. W., Thomson, N. R., Titball, R. W., Holden, M. T., Prentice, M. B., Sebaihia, M., James, K. D., Churcher, C., Mungall, K. L., Baker, S., Basham, D., Bentley, S. D., Brooks, K., Cerdeno-Tarraga, A. M., Chillingworth, T., Cronin, A., Davies, R. M., Davis, P., Dougan, G., Feltwell, T., Hamlin, N., Holroyd, S., Jagels, K., Karlyshev, A. V., Leather, S., Moule, S., Oyston, P. C., Quail, M., Rutherford, K., Simmonds, M., Skelton, J., Stevens, K., Whitehead, S., and Barrell, B. G. (2001) Genome sequence of *Yersinia pestis*, the causative agent of plague, *Nature 413*, 523−527.
45. Tamas, I., Klasson, L., Canback, B., Naslund, A. K., Eriksson, A. S., Wernegreen, J. J., Sandstrom, J. P., Moran, N. A., and Andersson, S. G. (2002) 50 million years of genomic stasis in endosymbiotic bacteria, *Science 296*, 2376−2379.
46. Shigenobu, S., Watanabe, H., Hattori, M., Sakaki, Y., and Ishikawa, H. (2000) Genome sequence of the endocellular bacterial symbiont of aphids *Buchnera* sp. APS, *Nature 407*, 81−86.
47. Xu, X., Matsuno-Yagi, A., and Yagi, T. (1993) DNA sequencing of the seven remaining structural genes of the gene cluster encoding the energy-transducing NADH-quinone oxidoreductase of *Paracoccus denitrificans*, *Biochim. Biophys. Acta 1141*, 1−17.
48. Dupuis, A., Peinnequin, A., Chevallet, M., Lunardi, J., Darrouzet, E., Pierrard, B., Procaccio, V., and Issartel, J. P. (1995) Identification of five *Rhodobacter capsulatus* genes encoding the equivalent of ND subunits of the mitochondrial NADH-ubiquinone oxidoreductase, *Gene 167*, 99−104.
49. Anderson, S., de Bruijn, M. H. L., Coulson, A. R., Eperon, I. G., Sanger, F., and Young, I. G. (1982) Complete sequence of bovine mitochondrial DNA, *J. Mol. Biol. 156*, 683−717.
50. Bibb, M. J., Van Etten, R. A., Wright, C. T., Walberg, M. W., and Clayton, D. A. (1981) Sequence and gene organization of mouse mitochondrial DNA, *Cell 26*, 167−180.
51. Ursing, B. M., and Arnason, U. (1998) The complete mitochondrial DNA sequence of the pig (*Sus scrofa*), *J. Mol. Evol. 47*, 302−306.
52. Hiendleder, S., Lewalski, H., Wassmuth, R., and Janke, A. (1998) The complete mitochondrial DNA sequence of the domestic sheep (*Ovis aries*) and comparison with the other major ovine haplotype, *J. Mol. Evol. 47*, 441−448.

BI0340346